

Supporting Information to

QM/MM STUDIES OF HAIRPIN RIBOZYME SELF-CLEAVAGE SUGGEST THE FEASIBILITY OF MULTIPLE COMPETING REACTION MECHANISMS

Vojtěch Mlýnský, Pavel Banáš, Nils G. Walter, Jiří Šponer, and Michal Otyepka

1) Parameters of reaction intermediates

Two pentahedral phosphorane intermediates (IN-*pro*-S_PH, IN-*pro*-R_PH) were used as non-standard residues in molecular dynamics (MD) simulations. The partial atomic charges for adenine/guanine (A/G) pentahedral intermediates protonated on *pro*-S_P or *pro*-R_P nonbridging oxygens were obtained by the restrained electrostatic potential (RESP) fit procedure at HF/6-31G(d) level of theory according to the scheme of Cornell *et al.*^{1,2} The model compound contained A/G pentahedral intermediate capped by 5'-methylphosphate and 3'-methylphosphate termini (Figure S1). The geometry of the A/G RNA strand carrying the pentahedral phosphorane was taken from our preliminary QM/MM calculations. This model was protonated on *pro*-S_P and *pro*-R_P nonbridging oxygens, respectively, and all hydrogen atoms were geometrically optimized at HF/6-31G(d) level of theory using the Gaussian03 program.³ All heavy atoms were fixed in their original positions. Subsequently, the partial atomic charges were determined using RESP procedure at HF/6-31G(d) level of theory. New residue was defined for A-1 and G+1 connected by pentahedral phosphorane. The obtained partial charges were used for atoms of sugar-phosphate backbone between A(C2', C3') and G(C4') carrying the pentahedral phosphorane, while the parm99 charges were used for the remaining atoms. The residual fractional charge was spread equally to all atoms of A/G intermediate residue. Non-zero van der Waals parameters ($r_0=0.6$ Å, $\sigma=0.0157$ kcal/mol) of hydrogen atom (HX) bound to non-bridging oxygen of the scissile phosphate together with P-OH-HX angle parameters ($k_\theta = 100$ kcal/molÅ², $\theta_0 = 108.5^\circ$) were used to retain a reasonable conformational behavior of protonated nonbridging oxygen in phosphorane intermediates. The other missing bonding parameters were derived by analogy from parm99 force field.

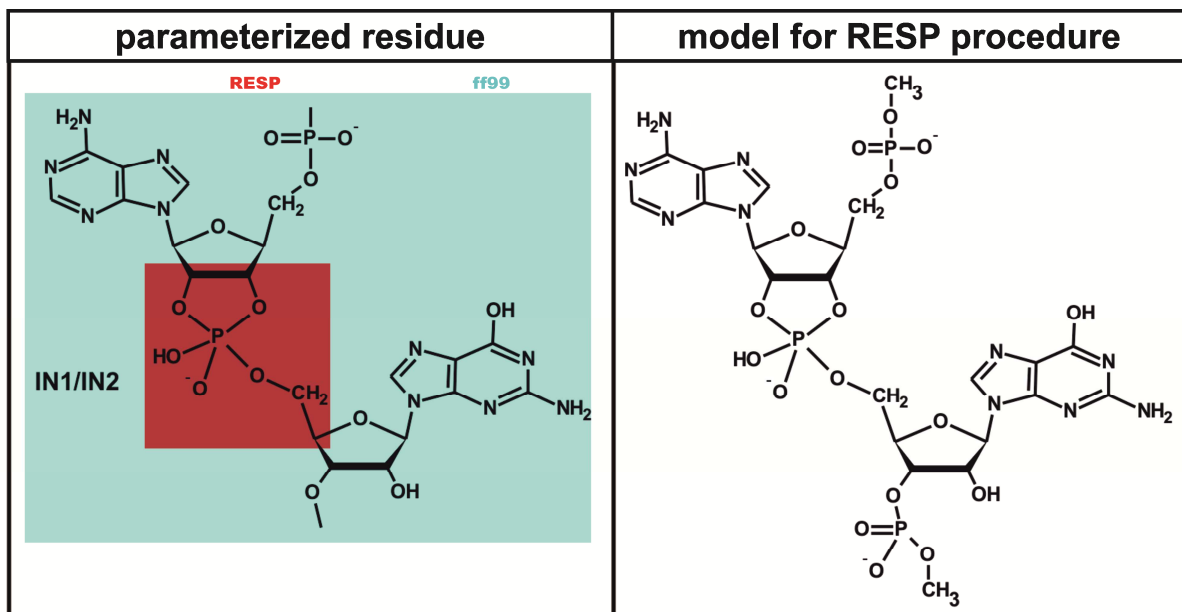


Figure S1: Left panel shows the structure of the non-standard residue and right panel the model, used for calculation of RESP charges. Whereas the green inset on the left panel illustrates atoms with default parm99 charges, the red inset shows atoms, which partial charges were derived from the RESP procedure.

a) AMBER prep file for phosphorane intermediate with protonated pro- S_P (OIP) oxygen (IN-pro- S_P H)

```

0      0      2

This is a remark line
molecule.res
IN1    XYZ    0
CHANGE  OMIT DU  BEG
0.0000
  1  DUMM  DU    M      999.000    999.0    -999.0    .00000
  2  DUMM  DU    M      999.000   -999.0     999.0    .00000
  3  DUMM  DU    M     -999.000    999.0     999.0    .00000
  4  P1    P     M      12.609000    1.116000    1.757000    1.15830
  5  O1P   O2    E      12.953000    2.380000    2.497000   -0.78390
  6  O2P   O2    E      11.729000    0.078000    2.381000   -0.78390
  7  O5'   OS    M      14.020000    0.387000    1.294000   -0.50680
  8  C5'   CT    M      14.082000   -0.919000   -0.052000    0.04790
  9  H5'1  H1    E       1.129000   -2.609000   -1.006000    0.06000
 10  H5'2  H1    E       2.668000   -2.564000   -1.854000    0.06000
 11  C4'   CT    M       2.766000   -1.848000    0.163000    0.09860
 12  H4'   H1    E       2.549000   -2.226000    1.153000    0.10950
 13  O4'   OS    S       4.209000   -1.769000    0.007000   -0.36270
 14  C1'   CT    B      17.346000   -0.004000   -0.468000    0.03150
 15  H1'   H2    E      17.904000   -0.122000   -1.397000    0.19280
 16  N9    N*    S      17.639000    1.363000    0.062000   -0.03300
 17  C8    CK    B      16.831000    2.254000    0.786000    0.19270
 18  H8    H5    E      15.778000    2.054000    0.918000    0.14740
 19  N7    NB    S      17.499000    3.303000    1.171000   -0.61520
 20  C5    CB    S      18.779000    3.188000    0.605000    0.04360
 21  C6    CA    B      20.023000    3.874000    0.619000    0.69300

```

22	N6	N2	B	20.319000	5.031000	1.153000	-0.90980
23	H61	H	E	21.182000	5.472000	0.869000	0.40360
24	H62	H	E	19.663000	5.604000	1.665000	0.40360
25	N1	NC	S	21.098000	3.367000	-0.036000	-0.76940
26	C2	CQ	B	21.019000	2.136000	-0.589000	0.57960
27	H2	H5	E	21.933000	1.880000	-1.103000	0.03940
28	N3	NC	S	19.855000	1.490000	-0.817000	-0.70760
29	C4	CB	E	18.818000	2.063000	-0.172000	0.29740
30	C3'	CT	M	2.237000	-0.397000	0.038000	0.01573
31	H3'	H1	E	1.932000	-0.180000	-0.976000	0.04001
32	C2'	CT	B	3.424000	0.490000	0.527000	0.30115
33	H2'1	H1	E	3.586000	1.355000	-0.106000	0.03906
34	O2'	OX	E	3.104000	0.896000	1.844000	-0.61791
35	O3'	OS	M	1.075000	-0.183000	0.856000	-0.24735
36	P2	P	M	1.298000	0.403000	2.441000	0.94910
37	O1P2	OH	S	1.941000	-0.613000	3.508000	-0.59197
38	H1P2	HX	E	1.215000	-0.919000	4.043000	0.43897
39	O2P2	O2	E	0.903000	1.853000	2.824000	-0.67713
40	O5x	OX	M	-0.540000	-0.205000	2.776000	-0.57352
41	C5x	CT	M	-1.068000	-1.504000	2.449000	-0.09649
42	H5x1	H1	E	-0.965000	-2.166000	3.310000	0.06973
43	H5x2	H1	E	-0.548000	-1.964000	1.617000	0.06973
44	C4x	CT	M	-2.587000	-1.429000	2.075000	0.41309
45	H4x	H1	E	-3.084000	-2.285000	2.519000	0.10950
46	O4x	OS	S	-3.261000	-0.264000	2.559000	-0.36270
47	C1x	CT	B	-3.993000	0.354000	1.501000	0.01120
48	H1x	H2	E	-4.958000	0.648000	1.885000	0.19270
49	N9b	N*	S	-3.293000	1.576000	1.010000	0.04130
50	C8b	CK	B	-2.203000	2.213000	1.550000	0.12950
51	H8b	H5	E	-1.662000	1.780000	2.366000	0.15610
52	N7b	NB	S	-1.760000	3.217000	0.837000	-0.57880
53	C5b	CB	S	-2.745000	3.381000	-0.143000	0.16650
54	C6b	C	B	-2.899000	4.363000	-1.188000	0.46910
55	O6b	O	E	-2.155000	5.293000	-1.522000	-0.56760
56	N1b	NA	B	-4.077000	4.224000	-1.888000	-0.48660
57	H1b	H	E	-4.237000	4.929000	-2.574000	0.33450
58	C2b	CA	B	-5.001000	3.270000	-1.637000	0.75780
59	N2b	N2	B	-6.074000	3.300000	-2.377000	-0.97510
60	H21b	H	E	-6.006000	3.653000	-3.305000	0.42850
61	H22b	H	E	-6.653000	2.494000	-2.287000	0.42850
62	N3b	NC	S	-4.884000	2.321000	-0.711000	-0.64020
63	C4b	CB	E	-3.732000	2.429000	0.018000	0.11430
64	C3x	CT	M	-2.823000	-1.502000	0.563000	0.19430
65	H3x	H1	E	-2.028000	-1.007000	0.023000	0.05360
66	C2x	CT	B	-4.130000	-0.717000	0.419000	0.05910
67	H2x1	H1	E	-4.252000	-0.287000	-0.562000	0.08930
68	O2x	OH	S	-5.264000	-1.520000	0.717000	-0.62180
69	HOx2	HO	E	-4.992000	-2.423000	0.601000	0.41070
70	O3x	OS	M	-2.932000	-2.853000	0.116000	-0.53250

LOOP

C1' C2'
C5 C4
C4 N9
O2' P2
C1x C2x
C4b C5b
C4b N9b

IMPROPER

C8 C4 N9 C1'

```

C6   H61   N6   H62
N7   N9    C8   H8
N1   N3    C2   H2
C5   N1    C6   N6
C8b  C4b   N9b  C1x
C5b  N1b   C6b  O6b
C6b  C2b   N1b  H1b
C2b  H21b  N2b  H22b
N7b  N9b   C8b  H8b
N1b  N3b   C2b  N2b

```

```

DONE
STOP

```

b) AMBER prep file for phosphorane intermediate with protonated pro-R_P (O2P) oxygen (IN-pro-R_PH)

```

0   0   2

```

```

This is a remark line
molecule.res

```

```

IN2   XYZ   0

```

```

CHANGE      OMIT DU   BEG

```

```

0.0000

```

1	DUMM	DU	M	999.000	999.0	-999.0	.00000
2	DUMM	DU	M	999.000	-999.0	999.0	.00000
3	DUMM	DU	M	-999.000	999.0	999.0	.00000
4	P1	P	M	12.609000	1.116000	1.757000	1.15809
5	O1P	O2	E	12.953000	2.380000	2.497000	-0.78411
6	O2P	O2	E	11.729000	0.078000	2.381000	-0.78411
7	O5'	OS	M	14.020000	0.387000	1.294000	-0.50701
8	C5'	CT	M	14.082000	-0.919000	-0.052000	0.04769
9	H5'1	H1	E	1.129000	-2.609000	-1.006000	0.05979
10	H5'2	H1	E	2.668000	-2.564000	-1.854000	0.05979
11	C4'	CT	M	2.766000	-1.848000	0.163000	0.09839
12	H4'	H1	E	2.549000	-2.226000	1.153000	0.10929
13	O4'	OS	S	4.209000	-1.769000	0.007000	-0.36291
14	C1'	CT	B	17.346000	-0.004000	-0.468000	0.03129
15	H1'	H2	E	17.904000	-0.122000	-1.397000	0.19259
16	N9	N*	S	17.639000	1.363000	0.062000	-0.03321
17	C8	CK	B	16.831000	2.254000	0.786000	0.19249
18	H8	H5	E	15.778000	2.054000	0.918000	0.14719
19	N7	NB	S	17.499000	3.303000	1.171000	-0.61541
20	C5	CB	S	18.779000	3.188000	0.605000	0.04339
21	C6	CA	B	20.023000	3.874000	0.619000	0.69279
22	N6	N2	B	20.319000	5.031000	1.153000	-0.91001
23	H61	H	E	21.182000	5.472000	0.869000	0.40339
24	H62	H	E	19.663000	5.604000	1.665000	0.40339
25	N1	NC	S	21.098000	3.367000	-0.036000	-0.76961
26	C2	CQ	B	21.019000	2.136000	-0.589000	0.57939
27	H2	H5	E	21.933000	1.880000	-1.103000	0.03919
28	N3	NC	S	19.855000	1.490000	-0.817000	-0.70781
29	C4	CB	E	18.818000	2.063000	-0.172000	0.29719
30	C3'	CT	M	2.240000	-0.405000	0.047000	0.02332
31	H3'	H1	E	1.938000	-0.196000	-0.971000	0.02685
32	C2'	CT	B	3.426000	0.487000	0.527000	0.32830
33	H2'1	H1	E	3.593000	1.339000	-0.126000	0.01660
34	O2'	OX	E	3.106000	0.906000	1.839000	-0.62827
35	O3'	OS	M	1.077000	-0.182000	0.861000	-0.26326
36	P2	P	M	1.299000	0.420000	2.440000	1.00501

37	O1P2	O2	E	1.941000	-0.585000	3.518000	-0.74579
38	O2P2	OH	S	0.904000	1.875000	2.807000	-0.56120
39	H2P2	HX	E	0.086000	1.827000	3.292000	0.45277
40	O5x	OX	M	-0.540000	-0.184000	2.779000	-0.62624
41	C5x	CT	M	-1.068000	-1.486000	2.465000	-0.10012
42	H5x1	H1	E	-0.947000	-2.120000	3.337000	0.10206
43	H5x2	H1	E	-0.541000	-1.945000	1.640000	0.10206
44	C4x	CT	M	-2.586000	-1.415000	2.089000	0.41103
45	H4x	H1	E	-3.084000	-2.265000	2.543000	0.10929
46	O4x	OS	S	-3.260000	-0.244000	2.561000	-0.36291
47	C1x	CT	B	-3.991000	0.363000	1.495000	0.01099
48	H1x	H2	E	-4.955000	0.665000	1.874000	0.19249
49	N9b	N*	S	-3.290000	1.579000	0.993000	0.04109
50	C8b	CK	B	-2.201000	2.221000	1.527000	0.12929
51	H8b	H5	E	-1.703000	1.766000	2.350000	0.15589
52	N7b	NB	S	-1.756000	3.218000	0.804000	-0.57901
53	C5b	CB	S	-2.741000	3.372000	-0.178000	0.16629
54	C6b	C	B	-2.894000	4.343000	-1.234000	0.46889
55	O6b	O	E	-2.149000	5.270000	-1.577000	-0.56781
56	N1b	NA	B	-4.071000	4.198000	-1.933000	-0.48681
57	H1b	H	E	-4.226000	4.892000	-2.631000	0.33429
58	C2b	CA	B	-4.995000	3.246000	-1.673000	0.75759
59	N2b	N2	B	-6.068000	3.269000	-2.415000	-0.97531
60	H21b	H	E	-6.011000	3.636000	-3.338000	0.42829
61	H22b	H	E	-6.651000	2.466000	-2.321000	0.42829
62	N3b	NC	S	-4.879000	2.306000	-0.738000	-0.64041
63	C4b	CB	E	-3.729000	2.422000	-0.009000	0.11409
64	C3x	CT	M	-2.820000	-1.503000	0.578000	0.19409
65	H3x	H1	E	-2.024000	-1.016000	0.034000	0.05339
66	C2x	CT	B	-4.127000	-0.720000	0.424000	0.05889
67	H2x1	H1	E	-4.250000	-0.299000	-0.562000	0.08909
68	O2x	OH	S	-5.261000	-1.519000	0.730000	-0.62201
69	HOx2	HO	E	-4.985000	-2.424000	0.634000	0.41049
70	O3x	OS	M	-2.930000	-2.859000	0.145000	-0.53271

LOOP

C1' C2'
C5 C4
C4 N9
O2' P2
C1x C2x
C4b C5b
C4b N9b

IMPROPER

C8 C4 N9 C1'
C6 H61 N6 H62
N7 N9 C8 H8
N1 N3 C2 H2
C5 N1 C6 N6
C8b C4b N9b C1x
C5b N1b C6b O6b
C6b C2b N1b H1b
C2b H21b N2b H22b
N7b N9b C8b H8b
N1b N3b C2b N2b

DONE

STOP

c) AMBER parm file with non-standard parameters

```
# force field modification for RMA, RGM, RGT, RAP, IN-pro-RpH, IN-pro-SpH, and L25 residues
MASS
OX          16.00    0.465 based on OS ether and ester oxygen
HX          1.008    0.135 based on HO hydroxyl group

BOND
CT-OX      320.0    1.410 based on CT-OS JCC,7,(1986),230; NUCLEIC ACIDS
OX-P       230.0    1.965 based on P-OS JCC,7,(1986),230; NA PHOSPHATES with changed distance
HX-OH     553.0    0.960 based on HO-OH JCC,7,(1986),230; SUGARS,SER,TYR
CQ-NA     502.0    1.324 based on CQ-NC JCC,7,(1986),230; ADE

ANGLE
H1-CT-OX   50.0    109.50 based on H1-CT-OS changed based on NMA nmodes
CT-CT-OX   50.0    109.50 based on CT-CT-OS
CT-OX-P    100.0   120.50 based on CT-OS-P
OX-P -OX   45.0    180.00 based on OS-P -OS with 180 degree instead of 45
OS-P -OX   45.0    90.00 based on OS-P -OS with 90 degree instead of 45
O2-P -OX   45.0    90.00 based on O2-P -OS with 90 degree instead of 45
OH-P -OX   45.0    90.00 based on OH-P -OS with 90 degree instead of 45
HX-OH-P    100.0   108.50 based on HO-OH-P with force constant 100kcal/molA2
CB-CA-NA   70.0    117.30 based on CB-CA-NC
NC-CQ-NA   70.0    129.10 based on NC-CQ-NC
H5-CQ-NA   50.0    115.45 based on H5-CQ-NC
CA-NA-CQ   70.0    118.60 based on CA-NC-CQ
CQ-NA-H    50.0    118.00 based on CA-NA-H changed based on NMA nmodes

DIHEDRAL
H1-CT-OX-P 3      1.15      0.0      3.      based on X-CT-OS-X JCC,7,(1986),230
CT-CT-OX-P 3      1.15      0.0      3.      based on X-CT-OS-X JCC,7,(1986),230
O2-P -OX-CT 1      0.25      0.0     -3.     based on OS-P-OS-CT JCC,7,(1986),230
O2-P -OX-CT 1      1.20      0.0      2.     based on OS-P-OS-CT gg&gt ene.631g*/mp2
OH-P -OX-CT 1      0.25      0.0     -3.     based on OS-P-OS-CT JCC,7,(1986),230
OH-P -OX-CT 1      1.20      0.0      2.     based on OS-P-OS-CT gg&gt ene.631g*/mp2
OS-P -OX-CT 1      0.25      0.0     -3.     based on OS-P-OS-CT JCC,7,(1986),230
OS-P -OX-CT 1      1.20      0.0      2.     based on OS-P-OS-CT gg&gt ene.631g*/mp2
OX-P -OX-CT 1      0.00      0.0      1.     this torsion should be zero in sp3d
OX-P -OS-CT 1      0.25      0.0     -3.     based on OS-P-OS-CT JCC,7,(1986),230
OX-P -OS-CT 1      1.20      0.0      2.     based on OS-P-OS-CT gg&gt ene.631g*/mp2
OX-CT-CT-OS 1      0.144     0.0     -3.     based on OS-CT-CT-OS parm98, TC,PC,PAK
OX-CT-CT-OS 1      1.175     0.0      2.     based on OS-CT-CT-OS Piotr et al.
H1-CT-CT-OX 1      0.25      0.0      1.     based on H1-CT-CT-OS Junmei et al, 1999
OX-CT-CT-OH 1      0.144     0.0     -3.     based on OS-CT-CT-OH parm98, TC,PC,PAK
OX-CT-CT-OH 1      1.175     0.0      2.     based on OS-CT-CT-OH parm98, TC,PC,PAK
X -NA-CQ- X 4      9.60      80.0     2.

NONBON
OX          1.6837    0.1700      based on OS OPLS ether
HX          0.6000    0.0157      based on HS W. Cornell CH3SH --> CH3OH FEP
```

2) Behavior of Reaction Intermediates

We performed four 50 ns-long MD simulations of all possible combinations of protonation state of the reaction intermediate and A38 adenine (protonated *pro-R_pH* or *pro-S_pH* nonbridging oxygen of phosphorane group with either canonical A38 or protonated A38H⁺ form). We used the same protocol for setting up MD's as in our previous MD study.⁴ MD simulations containing the canonical A38 are not further described as the A38 left the active site within the first ~4 ns of each MD simulation and exhibited the same behavior as reported recently in our MD paper.⁴ As a consequence, only two simulations with protonated A38H⁺ form are discussed below and were further used for preparation of the starting geometries for the following hybrid quantum mechanical/ molecular mechanical QM/MM study. We would like to note, that the bonding force field parameters for pentahedral phosphorane intermediate

residues were not thoroughly tested and therefore the results should be interpreted with care considering potential limitation of the force field used.

*G+1(*pro-S_pH*) intermediate with A38H⁺ (IN-*pro-S_pH*/G8/A38H⁺)*

The G8 nucleobase established the 4BPh (base-phosphate) contact with G+1 pentahedral phosphorane within first part of MD simulation (Figure S2C). This contact was weakened just for a limited time (for ~6 ns in overall) by reorientation of G8 within the active site and formation of transient G+1(*pro-S_pH*)...G8(O6) H-bond around ~33 and ~46 ns. The A9 nucleobase formed bifurcated A9(N6H)...A-1(O2')/G+1(*pro-R_p*) H-bond, temporary substituted (from ~38 to 46 ns) by the formation of the A10(N6H)...A-1(O2') H-bond by the neighboring A10 nucleobase (Figures S2A, S2C). The protonated A38H⁺ nucleobase established two stable A38H⁺(N6H)...G+1(*pro-R_p*) and A38H⁺(N1H)...G+1(O5') H-bonds to the pentahedral phosphorane (Figure S2C).

*G+1(*pro-R_pH*) intermediate with A38H⁺ (IN-*pro-R_pH*/G8/A38H⁺)*

The A-1(O2') oxygen lost immediately its interaction with G8 and established a new A10(N6H)...A-1(O2') H-bond within the first ns of MD simulation (Figure S2C). Thereby, G8 formed temporary bifurcated G8(N1H/N2H)...G+1(*pro-S_p*) H-bond. The protonated G+1(*pro-R_pH*) group established also bifurcated A38H⁺(N6H)...G+1(*pro-R_p*)/A9(N6H)...G+1(*pro-R_p*) H-bond (Figure S2C). Interestingly, we observed significant H-bond reorientation and a renewal of G8(N1H)...A-1(O2') and G8(N2H)...G+1(*pro-R_p*) H-bonds in the second part of MD simulation (Figures S2B, S2C).

The hydrogen on protonated G+1(*pro-R_pH*) group was not involved as a proton donor in any H-bond with surrounding bases and pointed either in the direction to the A-1 sugar (~75%), or the G+1 sugar (~25%). We did not observe any water mediated H-bond between G+1(O5') and G+1(*pro-R_pH*). In contrast to the previous IN-*pro-R_pH*/G8/A38H⁺ MD simulation, the A38H⁺(N6H)...G+1(*pro-R_p*) H-bond was significantly weakened (after ~25 ns) due to the reorientation of non-bridging oxygens of the pentahedral phosphorane and subsequent formation of the G8(N1H)...A-1(O2') and G8(N2H)...G+1(*pro-R_p*) H-bonds. Nevertheless, an average structure taken at the end of this simulation showed the best agreement with the X-ray structures (Figure S2B) of vanadate transition states analogs of the hairpin ribozyme (PDB code 1M5O, 2P7E).^{5,6}

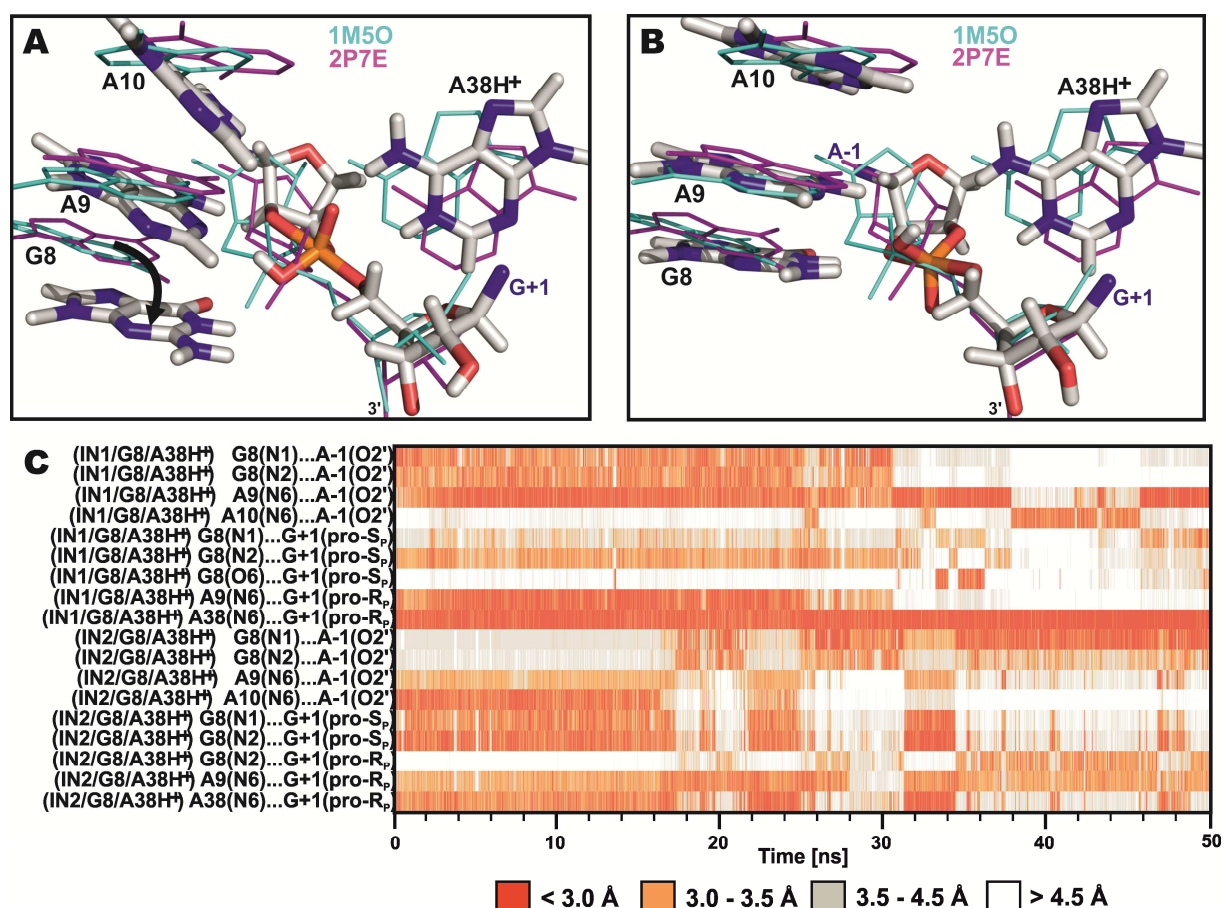


Figure S2: Last one ns average structures of the active site of *IN-pro-R_pH/G8/A38H⁺* (A) and *IN-pro-S_pH/G8/A38H⁺* (B) MD simulations (in sticks) of the hairpin ribozyme are superimposed with two crystal structures of vanadate TS analogs (1M50 in cyan, 2P7E in magenta lines). (A) The protonated *pro-S_pH* oxygen (*pro-S_pH*) causes reorientation of G8 (black arrow), A9 and A10 nucleobases in *IN-pro-R_pH/G8/A38H⁺* MD simulation. (B) On the other hand, the MD simulation of *IN-pro-S_pH/G8/A38H⁺* phosphorane intermediate shows the best agreement with the X-ray structures of vanadate TS analogs. (C) Time evolution of interactions of the G+1(O2') oxygen and protonated *pro-R_p*/*pro-S_p* oxygens with groups of neighboring nucleobases (IN1 and IN2 denote *IN-pro-S_pH* and *IN-pro-R_pH*, respectively).

3) Starting structures for QM/MM calculations

Snapshots from both *IN-pro-R_pH/G8/A38H⁺* and *IN-pro-S_pH/G8/A38H⁺* MD simulations were chosen based on geometrical arrangement of the protonated phosphorane with maximalized base-phosphate interaction (BPh)⁷ towards canonical G8 and protonated A38H⁺ residues. Further we reselected only those snapshots, where the protonated G+1(*pro-R_pH*) or G+1(*pro-S_pH*) non-bridging oxygen achieved the best orientation in the direction either of the A-1(O2') or the G+1(O5') oxygen. Finally, we considered 4 different MD snapshots (two with protonated G+1(*pro-R_p*) and other two with protonated G+1(*pro-S_p*) oxygen) that were subsequently used to prepare four starting structures for QM/MM calculations (Figure S3).

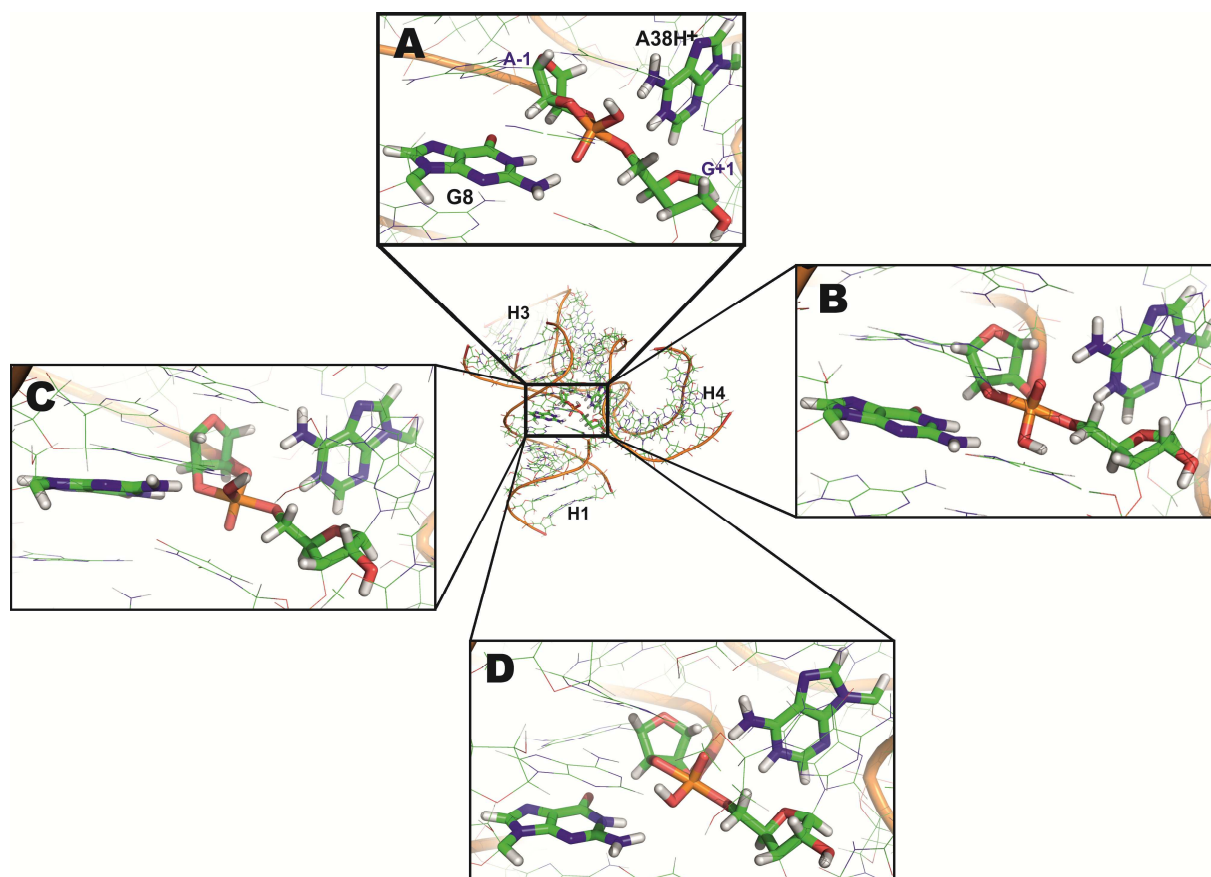


Figure S3: (A) Starting structure for QM/MM calculations taken from IN-pro-S_pH/G8/A38H⁺ MD simulation of the hairpin ribozyme. The protonated pentahedral phosphorane and key nucleobases within the active site are highlighted in sticks. Water molecules and counter ions are not shown for clarity. (B,C,D) Detailed view into the active site shows additional conformations of the pentahedral phosphorane and neighboring nucleobases, which were also considered as starting points for the subsequent QM/MM study.

Supporting tables:

Table S1: Summarized extrapolated CBS(T)^a energies (in kcal/mol, related to the reactant state), MPW1K/6-31+G(d,p) solvation energies, Gibbs Energy corrections and total Gibbs energies at the extrapolated CBS(T) level of the endo/exo-3'-(1'-amino-4'-methylribose)-5'-methylphosphodiester cleavage model. All geometries were optimized at CPCM ($\epsilon_r=78.4$)/MPW1K/6-31+G(d,p) level (see Methods in main text for details). The solvation term was calculated as the difference between CPCM($\epsilon_r=78.4$)/MPW1K/6-31+G(d,p) and gas phase MPW1K/6-31+G(d,p) SCF energies. The corrections to Gibbs energies were calculated at the CPCM($\epsilon_r=78.4$)/MPW1K/6-31+G(d,p) level.

endo (<i>pro-R_p</i>)	R	TS ₁	IN ₁	TS ₂	IN ₂	TS ₃	P	P'
CBS(T)	0.0	28.9	27.1	36.8	30.0	37.4	4.1	19.0
MPW1K solvation energy	0.0	-1.2	-4.5	-4.6	-5.2	-0.6	-1.4	-9.4
MPW1K Gibbs Energy correction	0.0	0.3	1.2	0.4	0.5	-2.2	-4.1	-12.9
CBS(T) Gibbs Energy in water	0.0	28.0	23.8	32.5	25.3	34.6	-1.4	-3.2
exo (<i>pro-S_p</i>)	R	TS ₁	IN ₁	TS ₂	IN ₂	TS ₃	P	P'
CBS(T)	0.0	27.1	21.7	32.4	26.6	37.9	4.1	19.0
MPW1K solvation energy	0.0	0.1	-1.6	-4.1	-3.4	-1.0	-1.4	-9.4
MPW1K Gibbs Energy correction	0.0	0.3	1.9	0.2	0.9	-2.2	-4.1	-12.9
CBS(T) Gibbs Energy in water	0.0	27.5	21.9	28.5	24.1	34.6	-1.4	-3.2

^a MP2/CBS energies corrected to higher-order correlation effects using CCSD(T) energies (see Methods section).

Table S2: List of the specific reaction mechanisms studied here and protonation states of key reaction participants G8, A38 and phosphate/phosphorane/cyclic phosphate, along respective reaction pathways (for names see Table 2 in main text). G8t stands for G8 enol tautomer, Ph for phosphate, Phr for phosphorane, cPh for cyclic phosphate.

Name	General base	General acid	R			IN/TS			P		
			G8	A38	Ph	G8	A38	Phr	G8	A38	cPh
$G^-/A^+/G8/A38H^+$	$G8^-$	$A38H^+$	$G8^-$	$A38H^+$	Ph^-	$G8$	$A38H^+$	Phr^{2-}	$G8$	$A38$	cPh^-
$pro-R_p/pro-R_p/G8/A38H^+$	$G+1(pro-R_p)$	$G+1(pro-R_p)$	$G8$	$A38H^+$	Ph^-	$G8$	$A38H^+$	Phr^-	$G8$	$A38H^+$	cPh^-
$pro-R_p/pro-R_p/G8t/A38H^+$	$G+1(pro-R_p)$	$G+1(pro-R_p)$	$G8t$	$A38H^+$	Ph^-	$G8t$	$A38H^+$	Phr^-	$G8t$	$A38H^+$	cPh^-
$pro-R_p/pro-R_p/G8/A38$	$G+1(pro-R_p)$	$G+1(pro-R_p)$	$G8$	$A38$	Ph^-	$G8$	$A38$	Phr^-	$G8$	$A38$	cPh^-
$pro-R_p/A^+/G8/A38H^+$	$G+1(pro-R_p)$	$A38H^+$	$G8$	$A38H^+$	Ph^-	$G8$	$A38H^+$	Phr^-	$G8$	$A38$	cPh
$pro-S_p/pro-S_p/G8/A38H^+$	$G+1(pro-S_p)$	$G+1(pro-S_p)$	$G8$	$A38H^+$	Ph^-	$G8$	$A38H^+$	Phr^-	$G8$	$A38H^+$	cPh^-
$pro-S_p/pro-S_p/G8t/A38H^+$	$G+1(pro-S_p)$	$G+1(pro-S_p)$	$G8t$	$A38H^+$	Ph^-	$G8t$	$A38H^+$	Phr^-	$G8t$	$A38H^+$	cPh^-
$pro-S_p/pro-S_p/G8/A38$	$G+1(pro-S_p)$	$G+1(pro-S_p)$	$G8$	$A38$	Ph^-	$G8$	$A38$	Phr^-	$G8$	$A38$	cPh^-

Table S3a: The MPW1K/6-31+G(d,p) gas phase energies, solvation and Gibbs Energy corrections (calculated at CPCM($\epsilon_r=78.4$)/MPW1K/6-31+G(d,p) level), and total Gibbs Energy profiles of the self-cleavage reaction of the endo/exo-3'-(1'-amino-4'-methylribose)-5'-methylphosphodiester sugar-phosphate backbone model extended by N9-methyl guanine and protonated N9-methyladenine. The proton of 2'-OH hydroxyl was shuttled via pro-R_P (endo path) or pro-S_P (exo path) non-bridging oxygen. All energies and energy corrections are in kcal/mol and are related to reactant state. No pK_a correction (see Methods section) for N1-protonated-N9-methyladenine was included in total Gibbs energies.

endo (pro-R _P)	R	TS ₁	IN ₁	TS ₂	IN ₂	TS ₃	P
MPW1K/6-31+G(d,p)	0.0	25.6	14.4	26.8	19.4	24.3	-9.1
Solvation energy	0.0	-2.2	2.1	-1.2	0.6	5.0	5.6
Gibbs Energy correction	0.0	0.0	-0.8	-1.5	-0.7	-1.9	-4.2
MPW1K Gibbs Energy in water	0.0	23.4	15.7	24.1	19.3	27.3	-7.7
exo (pro-S _P)	R	TS ₁	IN ₁	TS ₂	IN ₂	TS ₃	P
MPW1K/6-31+G(d,p)	0.0	23.7	3.4	13.5	10.5	16.4	-9.1
Solvation energy	0.0	-3.8	6.6	3.2	1.8	6.7	3.7
Gibbs Energy correction	0.0	-0.8	1.2	0.0	0.5	-2.4	-3.0
MPW1K Gibbs Energy in water	0.0	19.1	11.2	16.7	12.8	20.7	-8.4

Table S3b: The MPW1K/6-31+G(d,p) gas phase energies, solvation and Gibbs Energy corrections (calculated at CPCM($\epsilon_r=78.4$)/MPW1K/6-31+G(d,p) level), and total Gibbs Energy profiles of the self-cleavage reaction of the endo/exo-3'-(1'-amino-4'-methylribose)-5'-methylphosphodiester sugar-phosphate backbone model extended by N1-deprotonated-N9-methyl guanine and N1-protonated-N9-methyladenine. The deprotonated guanine acts as a general base, while the protonated adenine acts as a general acid. All energies and energy corrections are in kcal/mol and are related to reactant state. No pK_a corrections for N1-deprotonated-N9-methyl guanine and N1-protonated-N9-methyladenine were included in total Gibbs energies.

	R	TS	P
MPW1K/6-31+G(d,p)	0.0	0.2	-41.4
Solvation energy	0.0	13.5	33.8
Gibbs Energy correction	0.0	-0.1	-4.0
MPW1K Gibbs Energy in water	0.0	13.6	-11.6

Table S4a: The MPW1K/6-31+G(d,p) reaction barriers (in kcal/mol, related to the reactant state) obtained for geometries along various paths representing the proton shuttling and G8⁻ general base reaction mechanisms (for names see Table 2 in main text). No pK_a corrections (for deprotonated G8⁻ and protonated A38H⁺) and Gibbs energy corrections (see Methods section) were applied in this Table.

	R	TS ₁	IN ₁	TS ₂	IN ₂	TS ₃	P
<i>pro-R_p/pro-R_p/G8/A38H⁺</i>	0.0	18.9	2.0	9.0	3.3	4.3	-14.8
<i>pro-R_p/A⁺/G8/A38H⁺</i>	0.0	18.9	2.0	9.0	3.3	3.6	-5.3
<i>pro-R_p/pro-R_p/G8t/A38H⁺</i>	0.0	23.6	2.6	10.2	4.3	5.9	-11.1
<i>pro-R_p/pro-R_p/G8/A38</i>	0.0	20.5	4.8	14.4	5.2	14.1	-8.6
<i>pro-S_p/pro-S_p/G8/A38H⁺</i>	0.0	21.7	8.0	12.8	3.0	6.6	-10.7
<i>pro-S_p/pro-S_p/G8t/A38H⁺</i>	0.0	29.0	11.1	14.4	5.6	5.6	-7.6
<i>pro-S_p/pro-S_p/G8/A38</i>	0.0	24.0	14.9	18.1	8.3	13.9	-5.1
<i>G⁻/A⁺/G8⁻/A38H⁺</i>	0.0	15.0					-15.4

Table S4b: The BLYP/6-31G(d) energies (in kcal/mol, related to the reactant state) obtained from QM/MM calculations representing the proton shuttling and G8⁻ general base reaction mechanisms (for names see Table 2 in main text). No pK_a corrections (for deprotonated bG8⁻ and protonated A38H⁺) and Gibbs energy corrections (see Methods section) were applied in this Table.

	R	TS ₁	IN ₁	TS ₂	IN ₂	TS ₃	P
<i>pro-R_p/pro-R_p/G8/A38H⁺</i>	0.0	15.9	1.8	8.2	2.5	3.1	-12.8
<i>pro-R_p/A⁺/G8/A38H⁺</i>	0.0	15.9	1.8	8.2	2.5	2.6	-4.9
<i>pro-R_p/pro-R_p/G8t/A38H⁺</i>	0.0	20.7	1.9	9.0	3.6	3.7	-10.4
<i>pro-R_p/pro-R_p/G8/A38</i>	0.0	17.8	4.2	11.7	4.6	10.2	-8.0
<i>pro-S_p/pro-S_p/G8/A38H⁺</i>	0.0	18.3	7.4	11.2	2.4	4.1	-10.4
<i>pro-S_p/pro-S_p/G8t/A38H⁺</i>	0.0	25.7	10.3	12.9	4.7	4.9	-7.3
<i>pro-S_p/pro-S_p/G8/A38</i>	0.0	20.1	12.0	15.6	7.9	10.6	-4.1
<i>G⁻/A⁺/G8⁻/A38H⁺</i>	0.0	9.7					-15.2

Table S5a: The MPW1K/6-31+G(d,p) gas phase and extrapolated CBS(T) energies, MPW1K/6-31+G(d,p) solvation energies, Gibbs Energy corrections and total Gibbs energies at the extrapolated CBS(T) level of the endo/exo-3'-(1'-amino-4'-methylribose)-5'-methylphosphodiester cleavage model, where the endo (*pro-R_P*) non-bridging oxygen was thio-substituted. The proton of 2'-OH hydroxyl was shuttled via *pro-R_P* sulphur atom (endo path) or *pro-S_P* non-bridging oxygen (exo path). All energies and energy corrections are in kcal/mol and are related to reactant state. The solvation term was calculated as the difference between CPCM($\epsilon_r=78.4$)/MPW1K/6-31+G(d,p) and gas phase MPW1K/6-31+G(d,p) SCF energies. The corrections to Gibbs energies were calculated at the CPCM ($\epsilon_r=78.4$)/MPW1K/6-31+G(d,p) level.

endo (<i>pro-R_P</i>)	R	TS ₁	IN ₁	TS ₂	IN ₂	TS ₃	P	P'
MPW1K/6-31+G(d,p)	0.0	43.6	33.1	41.1	32.7	44.6	1.3	15.0
CBS(T)	0.0	40.7	30.4	38.2	30.2	44.1	3.5	17.6
Solvation energy	0.0	-2.7	-4.5	-4.0	-4.2	-1.0	-1.5	-9.0
Gibbs Energy correction	0.0	-2.6	-0.1	-1.1	-0.6	-3.3	-4.1	-12.5
CBS(T) Gibbs Energy in water	0.0	35.4	25.8	33.2	25.4	39.8	-2.1	-3.8
exo (<i>pro-S_P</i>)	R	TS ₁	IN ₁	TS ₂	IN ₂	TS ₃	P	P'
MPW1K/6-31+G(d,p)	0.0	27.5	19.2	29.4	23.9	36.8	1.3	15.0
CBS(T)	0.0	27.5	20.0	30.2	24.8	38.2	3.5	17.6
Solvation energy	0.0	-0.1	-2.6	-5.1	-4.7	-0.8	-1.5	-9.0
Gibbs Energy correction	0.0	0.6	1.8	1.4	2.1	-1.9	-4.1	-12.5
CBS(T) Gibbs Energy in water	0.0	28.0	19.2	26.4	22.2	35.5	-2.1	-3.8

Table S5b: The computed energies and corrections of the endo/exo-3'-(1'-amino-4'-methylribose)-5'-methylphosphodiester cleavage model, where the *pro-S_P* non-bridging oxygen was thio-substituted. The proton of 2'-OH hydroxyl was shuttled via *pro-R_P* non-bridging oxygen (exo path) or *pro-S_P* sulphur atom (exo path). The energies and corrections were computed by the same methodology as in Table S5a.

endo (<i>pro-R_P</i>)	R	TS ₁	IN ₁	TS ₂	IN ₂	TS ₃	P	P'
MPW1K/6-31+G(d,p)	0.0	31.8	25.5	33.9	28.7	38.3	5.7	15.4
CBS(T)	0.0	31.5	26.3	33.6	29.2	39.4	6.9	17.6
Solvation energy	0.0	-1.8	-5.5	-4.9	-6.2	-0.8	-2.3	-8.5
Gibbs Energy correction	0.0	-0.5	1.4	0.2	0.8	-2.9	-5.7	-13.3

CBS(T) Gibbs Energy in water	0.0	29.2	22.2	28.9	23.8	35.8	-1.1	-4.2
exo (<i>pro-S_P</i>)	R	TS ₁	IN ₁	TS ₂	IN ₂	TS ₃	P	P'
MPW1K/6-31+G(d,p)	0.0	42.0	28.2	37.9	32.8	46.0	5.7	15.4
CBS(T)	0.0	39.2	25.6	34.6	30.3	44.8	6.9	17.6
Solvation energy	0.0	-1.2	-1.4	-4.6	-3.5	-1.0	-2.3	-8.5
Gibbs Energy correction	0.0	-3.3	-0.8	-2.7	-1.7	-4.0	-5.7	-13.3
CBS(T) Gibbs Energy in water	0.0	34.7	23.4	27.3	25.1	39.8	-1.1	-4.2

Table S5c: The computed energies and corrections of the endo/exo-3'-(1'-amino-4'-methylribose)-5'-methylphosphodiester cleavage model, where both *pro-R_P* and *pro-S_P* non-bridging oxygens were thio-substituted. The proton of 2'-OH hydroxyl was thereby shuttled via *pro-R_P* (exo path) or *pro-S_P* (exo path) sulphur atoms. The energies and corrections were computed by the same methodology as in Table S5a.

endo (<i>pro-R_P</i>)	R	TS ₁	IN ₁	TS ₂	IN ₂	TS ₃	P	P'
MPW1K/6-31+G(d,p)	0.0	45.0	31.4	39.3	31.3	43.7	4.3	13.3
CBS(T)	0.0	43.0	29.4	37.0	29.3	43.6	5.9	16.3
Solvation energy	0.0	-4.6	-5.3	-4.6	-5.2	-1.8	-1.9	-7.7
Gibbs Energy correction	0.0	-2.3	0.0	-0.9	-0.7	-2.8	-4.5	-13.0
CBS(T) Gibbs Energy in water	0.0	36.1	24.0	31.6	23.5	39.1	-0.5	-4.4
exo (<i>pro-S_P</i>)	R	TS ₁	IN ₁	TS ₂	IN ₂	TS ₃	P	P'
MPW1K/6-31+G(d,p)	0.0	41.4	25.1	34.4	30.1	46.8	4.3	13.3
CBS(T)	0.0	39.4	23.5	31.6	28.3	46.2	5.9	16.3
Solvation energy	0.0	-2.5	-2.1	-3.8	-4.4	-3.5	-1.9	-7.7
Gibbs Energy correction	0.0	-2.4	-0.1	-1.3	-1.1	-2.9	-4.5	-13.0
CBS(T) Gibbs Energy in water	0.0	34.5	21.3	26.5	22.7	39.9	-0.5	-4.4

Supporting figures:

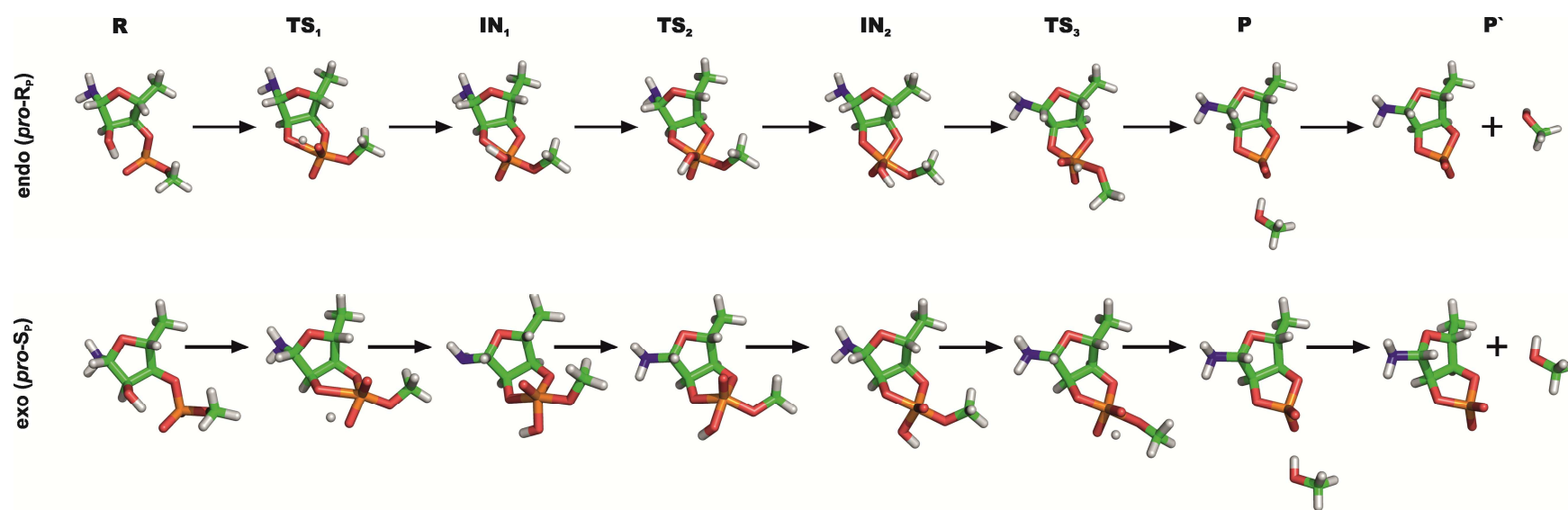


Figure S4: The structures along the reaction path of the endo/exo-3'-(1'-amino-4'-methylribose)-5'-methylphosphodiester self-cleavage reaction.

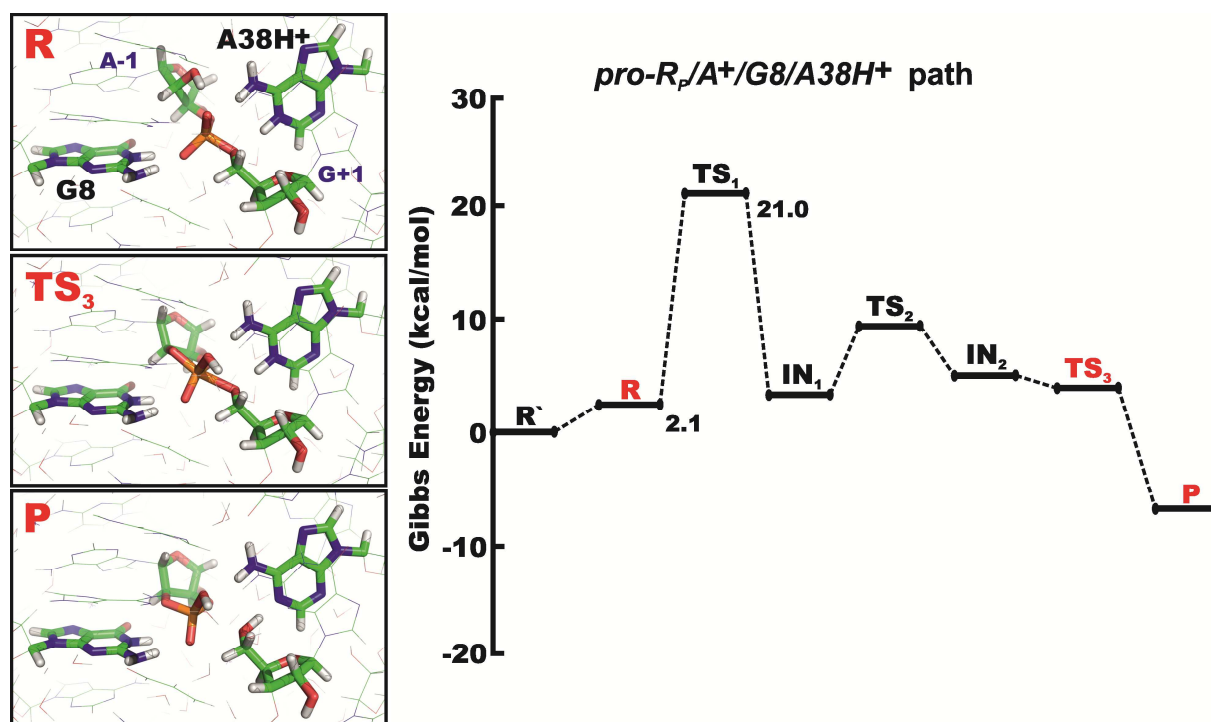


Figure S5: The Gibbs Energy profile of the *pro-R_p/A⁺/G8/A38H⁺* mechanism with A38H⁺ acting as a general acid. Structures in boxes show detailed view into the active site (QM core is highlighted in sticks) of the reactant, transition and product states (R, TS₃ and P) along the reaction pathway. All energies are relative to the R' state that represents the reactant with the dominant protonation states of G8 and A38 at pH ~7, i.e. both nucleobases in canonical forms.

References:

- (1) Cornell, W. D.; Cieplak, P.; Bayly, C. I.; Kollman, P. A. *J. Am. Chem. Soc.* **1993**, *115*, 9620-9631.
- (2) Cornell, W. D.; Cieplak, P.; Bayly, C. I.; Gould, I. R.; Merz, K. M.; Ferguson, D. M.; Spellmeyer, D. C.; Fox, T.; Caldwell, J. W.; Kollman, P. A. *J. Am. Chem. Soc.* **1995**, *117*, 5179-5197.
- (3) Frisch, M. J.; Trucks, G. W.; Schlegel, H. B.; Scuseria, G. E.; Robb, M. A.; Cheeseman, J. R.; Montgomery, Jr., J. A.; Vreven, T.; Kudin, K. N.; Burant, J. C. et al. Gaussian 03; Gaussian, Inc.: Pittsburgh, 2003.
- (4) Mlynsky, V.; Banas, P.; Hollas, D.; Reblova, K.; Walter, N. G.; Sponer, J.; Otyepka, M. *J. Phys. Chem. B* **2010**, *114*, 6642-6652.
- (5) Rupert, P. B.; Massey, A. P.; Sigurdsson, S. T.; Ferre-D'Amare, A. R. *Science* **2002**, *298*, 1421-1424.
- (6) Torelli, A. T.; Krucinska, J.; Wedekind, J. E. *RNA* **2007**, *13*, 1052-1070.
- (7) Zirbel, C. L.; Sponer, J. E.; Sponer, J.; Stombaugh, J.; Leontis, N. B. *Nucleic Acids Res.* **2009**, *37*, 4898-4918.